

AEROACOUSTIC PREDICTION OF AN AUTOMOTIVE COOLING FAN

Stéphan Magne¹, Stéphane Moreau¹, Alain Berry¹ and Marlène Sanjose¹

¹GAUS, Dept. of Mechanics, Université de Sherbrooke, Québec, Canada, J1K 2R1, Stephan.Magne@USherbrooke.ca

1. INTRODUCTION

The acoustic noise from low-speed cooling fans can be divided into two contributions: tonal noise and broadband noise. The latter is associated with the turbulence in the flow whereas the former is generated by the periodic components of the blade loads. Both have significant impact on the overall acoustic radiation, but for the human hearing, the tonal noise is a major annoyance and is, consequently, a prior challenge for manufacturers.

By installing a periodical circular obstruction at the inlet of a fan, Gérard *et al.* [1] have shown that the induced flow distortion is able to reduce the tonal noise. Although both analytical and experimental approaches have been carried out on this method, the aeroacoustic mechanisms have not yet been fully understood. As a first step to achieve a direct aerodynamic simulation of the interaction between a rotor and an obstruction, the aeroacoustic prediction of a single rotor in a typical fan test configuration is first studied.

2. AERODYNAMIC SIMULATION

2.1 Numerical configuration

The fan considered here is a typical automotive cooling fan on which both experimental and numerical data exist [2-4]. It is a 9-blade axial fan containing an L-shaped rotating ring and a short hub. Both the flow rate and the rotational speed are chosen to match the nominal point of this machine, respectively 2500 m³/h and 2500 rpm. The 380 mm outer diameter implies typical Mach number up to 0.15 at the blade tip (low subsonic), with a Reynolds number based on the chord of about 1.5×10^5 at midspan (transient turbulent regime). In this configuration, the rotor is flushed mounted on a plenum wall, as it is in a typical fan performance test bench.

In order to reduce the computational cost, only one blade passage is meshed and a uniform blade distribution is therefore assumed. Two multi-block structured meshes are generated using *Gridgen* for a total of 5.2 million nodes. Both have the same fine grid distribution, which was shown to yield proper wall resolution with *CFX*. Despite the same number of nodes, the “thin” mesh is more refined in the blade tip region, where the y^+ criterion is kept under 8 on the blade surfaces.

The resolution of the unsteady 3D compressible Reynolds Averaged Navier-Stokes equations is performed by the code *Turb'Flow* dedicated to turbomachinery and developed at Ecole Centrale de Lyon. The discretization of the equations is performed by a 2nd order spatial centered scheme of Jameson and a Runge-Kutta temporal scheme with 5 steps. The flow rate is imposed at the inlet of the domain on a spherical plenum, feeding the rotor uniformly. Downstream,

a porous domain is set to ensure a positive axial flow at the outlet, where the pressure is imposed with a radial equilibrium. The initial aerodynamic field is generated analytically with a uniform field and a steady RANS simulation is carried out in order to reduce the convergence duration. Once the aerodynamic field is established, a constant global time step is set to achieve the unsteady simulation. To preserve the stability of the schemes the time step is set to 8.9×10^{-8} s for the “thin” mesh and 5.3×10^{-8} s for the “coarse” mesh. The convergence is checked by monitoring the pressure and the flow rate on different surfaces along the simulation domain.

2.2 Aerodynamic results

The validation of the overall fan performance is achieved by comparing the static pressure rise across the rotor with the previous simulations and experimental data, shown as a bandwidth that accounts for the moulding and prototyping variability. On this short computational domain, the total pressure rise is taken between two planes close to the rotor. In Figure 1, the present result shows a very good agreement with existing experimental and numerical data.

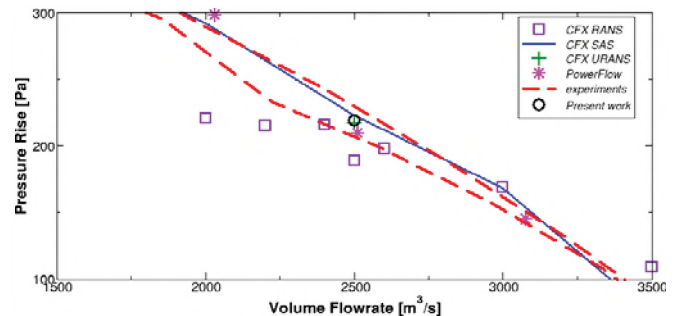


Figure 1: Fan performance.

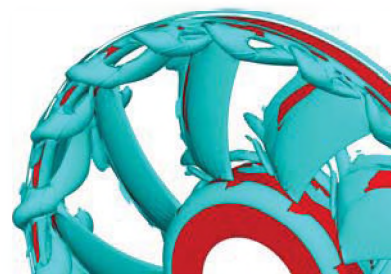


Figure 2: Iso-surface of the Q -factor on the rotor (all the other surfaces being hidden), “thin” mesh.

As observed previously [5], the dominant flow unsteadiness can be observed at the rotor tip. In Figure 2, the nature of the flow is very well highlighted by the Q -factor (a vortex identification technique). As a matter of fact, the pressure rise across the fan creates a flow recirculation in the tip clearance. This recirculation interacts with the rotor leading-edge and generates an unsteady blade load. In the present configuration, two tip vortices can be seen for each blade

passage, rotating at about 500 rpm. A speed reduction is thus observed in the tip clearance between the downstream and the upstream flow. Besides, this speed difference implies that each blade impacts a vortex structure at the frequency $f = N_{\text{vortices}} \times \Omega_{\text{relative}} = 600 \text{ Hz}$.

3. ACOUSTIC PREDICTION

3.1 Acoustic solver

The acoustic radiation is computed by a Ffowcs-Williams and Hawkins analogy based on the near field fluctuations provided by the aerodynamic simulation. The code *Foxhawk*, developed by Casalino [6], is used for this purpose. Taking advantage of the forward-time formulation of the FW-H equation, this code allows a concurrent flow/noise simulation. The transient pressure on the blade surfaces is imported and *Foxhawk* generates automatically the complete rotor configuration before the acoustic integrations, taking into account the phase delay between each blade. Considering the Mach numbers at the blade tip, only the thickness noise and the loading noise are computed and the effects of the quadrupole noise are neglected.

The acoustic pressure fluctuations are computed at 26 microphones equally distributed on a sphere, each being 1 m away from the rotor centre. Considering the blade passage frequency at 375 Hz, this distance can be considered as the far field.

3.2 Acoustic results

Only 3 blade passage periods were recorded for the purpose of this paper. Although this short duration cannot yet yield well resolved tones, it shows the correct trend. The sound pressure level at each microphone shows a dipole-like directivity with a maximum on the rotor axis. Moreover, the integration of the acoustic intensity over the sphere leads to an excellent prediction of the total emitted acoustic power: 82 and 83 dB for the “coarse” and the “thin” meshes respectively, compared to $82 \pm 2 \text{ dB}$ measured in a reverberant wind tunnel.

The power spectral density of the acoustic pressure at two microphones is presented in Figures 3 and 4, one microphone being on the rotor axis and the other in the rotor

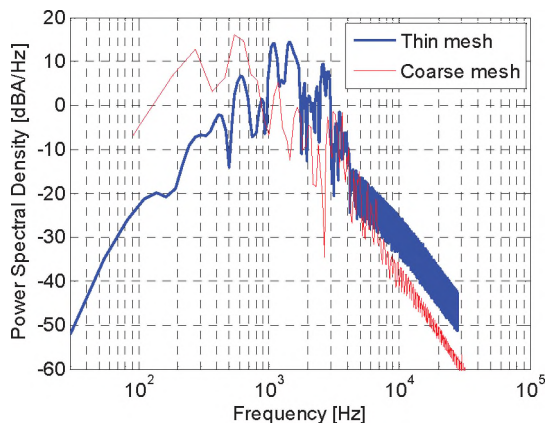


Figure 3: Microphone at 1 m on the rotor axis.

plane. The results for both meshes confirm the predicted tone at the frequency of the impact between the tip recirculation structure and the blades (600 Hz). However, several harmonics now appear in the “thin” mesh spectrum up to 3 kHz, which suggests a better resolution of the flow structures near the blade tip. Besides, the two tip vortices per blade passage are more dissimilar for the “coarse” mesh, yielding a more powerful peak at 300Hz. All these tones are also present in the experimental measurements [4].

4. CONCLUSION

Aerodynamic simulation of an automotive fan has been successfully achieved. This computation has highlighted the dominant flow structures that are the dominant sources of unsteadiness on the rotor surfaces and therefore the major sources of noise. As a second step, acoustic prediction has been performed using an acoustic analogy based on the static pressure fluctuation on the blades. A very good agreement is found with the experimental measurements both on the tonal content and the acoustic power emitted.

Future work will include a longer recording period which will lead to a more accurate acoustic prediction. Finally, an obstruction will be placed upstream the fan and aeroacoustic mechanisms will be studied in further details.

REFERENCES

- [1] Gérard A., Berry A., Masson P., Gervais Y. (2009). Modelling of tonal noise control from subsonic axial fans using flow control obstructions. *Journal of Sound and Vibration*, 321(1-2), 26-44.
- [2] Foss J., Neal D., Henner M., & Moreau S. (2001). *Evaluating CFD Models of Axial Fans by Comparisons with Phase-Averaged Experimental Data*. In Vehicle Thermal Management Systems.
- [3] Moreau S., Sanjose M., Magne S., & Henner M. (2011). *Unsteady Turbulent Simulations of Low-Speed Axial Fans*. In 46th Symposium of Applied Aerodynamics (3AF).
- [4] Pérot F., Kim M., Moreau S., Henner M., & Neal D. (2010). *Direct Aeroacoustics Prediction of a Low Speed Axial Fan*. In 16th AIAA/CEAS Aeroacoustics Conference.
- [5] Moreau S., Henner M., & Neal D. (2005). *3D Rotor-Stator Interaction in Automotive Engine Cooling Fan Systems*. In European Turbomachine Conference.
- [6] Casalino D. (2003). An advanced time approach for acoustic analogy predictions. *Journal of Sound and Vibration*, 261(4).

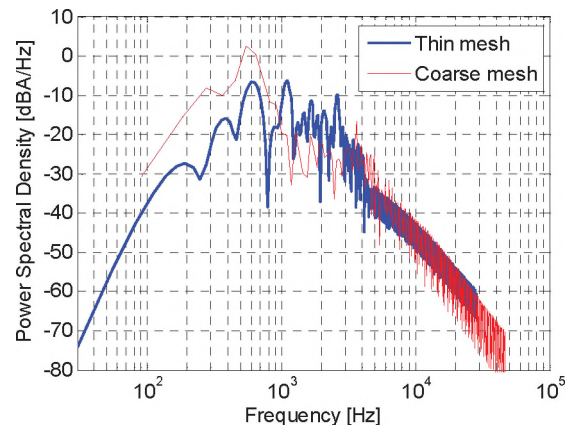


Figure 4: Microphone at 1 m in the rotor plane.